

In Situ Ordering of FePt Thin Films by Using Ag/Si and Ag/Mn₃Si/Ag/Si Templates

Yu-Nu Hsu, Sangki Jeong, David N. Lambeth, and David E. Laughlin

Abstract—*In situ* ordering of FePt thin films by sputtering onto Ag/Si and Ag/Mn₃Si/Ag/Si templates has been demonstrated. Due to the evolution from island-like to a continuous film structure as a function of Ag thickness, the ordering and orientation of the FePt films both change with Ag thickness. A continuous (002) Ag film results in a greater L1₀ phase formation with *c*-axis oriented both perpendicular to and in the film plane while the island-like Ag template results in less L1₀ phase formation, but a preferential *c*-axis orientation in the film plane. On the other hand, the FePt films deposited onto the Ag/Mn₃Si/Ag/Si template have their *c* axes aligned perpendicular to the film plane.

Index Terms—Ag underlayer, FePt film, high-*K_u* magnetic recording thin film, Mn₃Si underlayer, epitaxial growth.

I. INTRODUCTION

RECENTLY, due to the large magnetocrystalline anisotropy of the ordered tetragonal L1₀ FePt phase, FePt thin films have drawn considerable attention as a potential high-density magnetic recording material. It has been reported that L1₀ FePt thin films can be directly formed on MgO single crystal substrates by molecular beam epitaxy (MBE) [1], sputter-deposition [2] as well as by annealing Fe/Pt multilayers [3]. In this work, *in situ* ordering of the FePt thin films deposited at elevated temperature on Ag layers has been demonstrated. *In situ* ordering of the FePt films is partially induced by the small lattice misfits (5.2%) of the FePt (100)/Ag (100) planes. Single crystal Si (100) substrates were used to induce epitaxial growth of the Ag(100) thin film based on the orientational relationship of Ag(001)[110]||Si(001)[110] as reported by Yang *et al.* [4]. Moreover, our previous study [5] has shown that Mn₃Si can grow epitaxially on a Ag thin film, and here it is observed that both Ag/Si and Ag/Mn₃Si/Ag/Si templates can be used to obtain *in situ* ordered FePt thin films. In order to further understand the *in situ* ordering, the microstructural and magnetic properties of thin films grown on these two templates were investigated.

II. EXPERIMENTS

The FePt/Ag and FePt/Ag/Mn₃Si/Ag films were deposited on single crystal Si(100) substrates by RF diode sputtering in a Leybold-Heraeus Z-400 system. To remove the oxide layers, the Si (100) substrates were hydrofluoric acid (HF)-etched [4].

Manuscript received February 12, 2000. This work was supported by the Data Storage Systems Center at CMU under Grant ECD-89-07068 from National Science Foundation.

The authors are with Carnegie Mellon University, Pittsburgh, PA 15213 USA (e-mail: yh2a@andrew.cmu.edu).

Publisher Item Identifier S 0018-9464(00)08863-4.

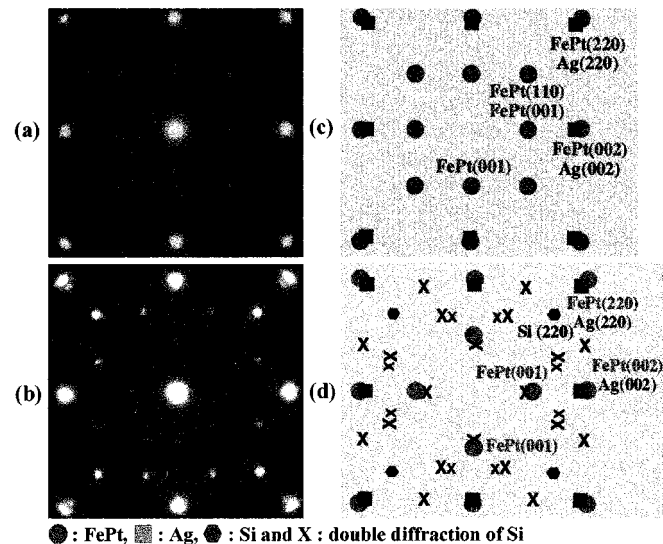


Fig. 1. TEM selected area diffraction patterns of the (a) FePt(30 nm)/Ag (175 nm) film, (b) FePt(30 nm)/Ag(10 nm) film and simulated patterns of the (c) FePt(30 nm)/Ag(175 nm) film and (d) FePt(30 nm)/Ag(10 nm) film.

The base pressure was 6×10^{-7} torr. The atomic composition of the FePt film deposited from a composite target was measured by X-ray fluorescence to be Fe₅₅Pt₄₅. The Ag and Mn₃Si films were deposited at 300°C with a fixed argon pressure of 10 mtorr, RF power density of 2.3 W/cm² and 6.9 W/cm², respectively. The FePt magnetic layers were deposited at sputtering power density of 0.5 W/cm², 300°C, and 2.5 mtorr. The thickness of FePt and Mn₃Si films was fixed at 30 nm and 400 nm, respectively. The Ag thickness was varied. The orientational relationships of these thin films were studied by $\theta/2\theta$ Rigaku X-ray diffractometer with Cu K α radiation as well as with a Philips EM 420T transmission electron microscope (TEM). The magnetic properties of the thin films were measured using an alternating gradient magnetometer (AGM) with fields up to 13 KOe.

III. RESULTS AND DISCUSSIONS

The TEM selected area diffraction (SAD) patterns and the simulated patterns of the 30 nm FePt deposited onto the 10 nm and 175 nm Ag underlayers are presented in Fig. 1. The orientational relationship of the FePt/Ag films is seen to be FePt(001)[110]||Ag(001)[110]. The L1₀ FePt 001 superlattice reflections are observed for these two Ag thickness, indicating that some *in situ* ordering of the L1₀ FePt thin film occurs independently of the Ag underlayer thickness. However, the L1₀ FePt 110 reflections observed in the diffraction pattern of the FePt/Ag (175 nm) film are not seen in that of the FePt/Ag (10 nm) thin film. The L1₀ FePt 110 reflections result from the

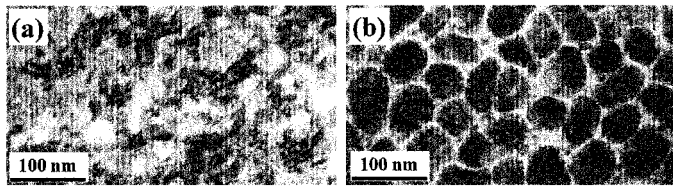


Fig. 2. TEM bright-field image of the FePt(30 nm)/Ag(10 nm) thin film.

FePt (001)-oriented grains. On the other hand, the $L1_0$ FePt 001 reflections are due to either the (100) or (010)-oriented grains. The absence of the $L1_0$ FePt 110 reflection in the FePt/Ag (10 nm) thin film shows that this FePt thin film has c -axes oriented in the thin film plane. The FePt/Ag (175 nm) thin film has its c -axes both parallel and perpendicular to the thin film plane because both the 110 and 001 reflections are observed in Fig. 1(a). Four $L1_0$ FePt 001 reflections are observed at these two Ag thickness, indicating the presence of the (100) and (010) oriented $L1_0$ grains. The $L1_0$ FePt superlattice reflection intensity of the FePt/Ag (10 nm) thin film is weaker than that of the FePt/Ag (100 nm) thin film. This suggests that the FePt deposited onto the 10 nm Ag underlayer is less ordered than that deposited onto the 175 nm thick Ag layer.

The overlap of the FePt and Ag (002) reflections in the diffraction pattern indicates a small lattice misfit between the FePt (001) and Ag (001) planes. In addition, the FePt $L1_0$ ordered and fcc disordered reflections can not be distinguished in Fig. 1. This shows that the lattice parameter values of these two phases are very close. The reflections marked as X in the simulated diffraction pattern are due to the double diffraction phenomena.

A TEM bright-field images of the FePt(30 nm)/Ag(175 nm) and FePt(30 nm)/Ag(10 nm) thin film are shown in Fig. 2. The FePt/Ag(10 nm) film reveals a particle-like microstructure. This results from the microstructure of the Ag underlayer which may be due to the incomplete wetting on the substrate. We believe thin Ag forms 3D islands on the substrate to cause the FePt deposits onto the Ag islands forming particle-like microstructure. For the thicker Ag films, the islands start to touch each other and form a continuous film. Therefore, the FePt thin film deposited onto the 175 nm Ag underlayer is a more continuous thin film.

The X-ray diffraction spectra of the 30 nm FePt film deposited at the Ag underlayers of various thickness are shown in Fig. 3(a). At thin Ag thickness (10 nm), the $L1_0$ FePt 001 peak is not observed. Based on the observation on the TEM SAD pattern (Fig. 2(b)), the absence of the $L1_0$ FePt 001 peak is attributed to the lack of (001)-oriented FePt grains on the 10 nm Ag underlayer.

As the Ag thickness increases to 100 nm, the $L1_0$ FePt 001 X-ray peak starts to appear, indicating that some $L1_0$ FePt (001)-oriented grains have formed. Comparing the positions of the $L1_0$ FePt 001 peaks for the films with 100 nm and 175 nm Ag, the 175 nm Ag has the $L1_0$ FePt 001 peak shifted to a higher angle. In addition, the 2θ X-ray peak between 46° and 50° shifts to higher angles as the Ag thickness increases. At the Ag thickness of 100 nm, the 2θ peak between 46° and 50° splits into two peaks, as shown in Fig. 2(a). Assuming the lattice parameter of a axis of disordered and ordered FePt are about the same, the peak between 46° and 50° can be deconvoluted as the $L1_0$ FePt 200

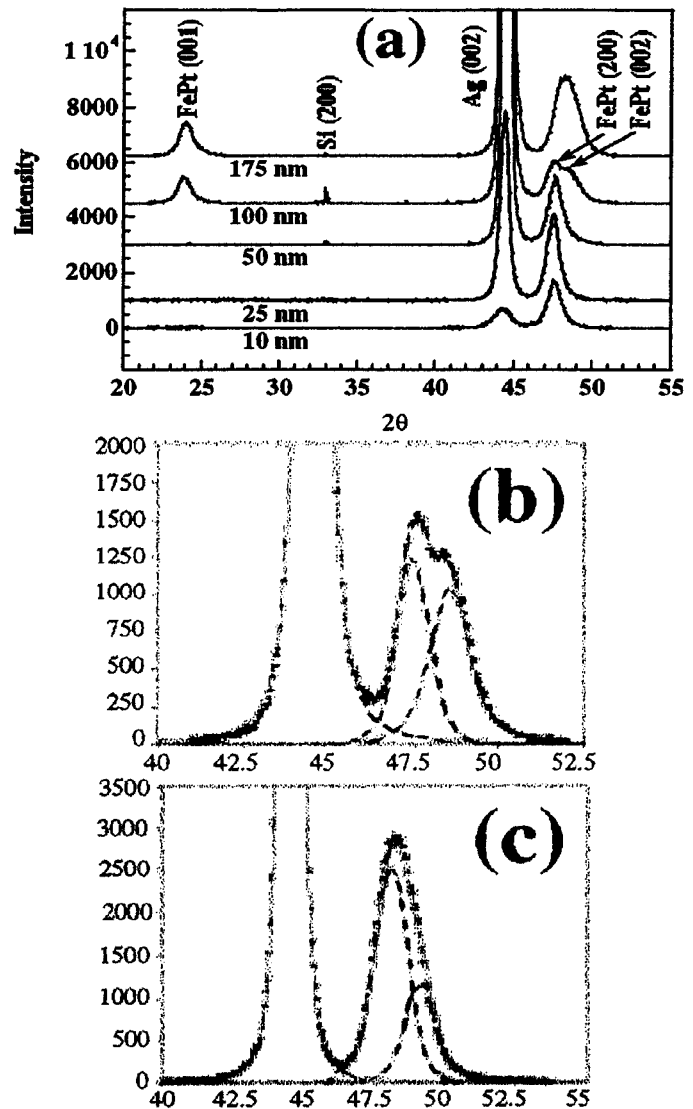


Fig. 3. (a) The X-ray $\theta/2\theta$ diffraction spectra of the FePt (30 nm)/Ag (x nm) thin films deposited onto the HF-etched Si (100) single crystal substrates and the deconvolution of the X-ray diffraction peaks of the (b) FePt(30 nm)/Ag (100 nm) and (c) FePt(30 nm)/Ag(175 nm) thin films.

and 002 peaks in Fig. 3(b). The peak position of the FePt 002 peak is fixed at 48.32° as deduced from the peak position of the FePt 001. The peak position of the FePt 200 after deconvolution is calculated as 47.50° . At the Ag thickness of 175 nm, the broad peak between 46° and 50° is composed of two peaks and can again be deconvoluted into the $L1_0$ FePt 200 and 002 peaks as shown in Fig. 3(c). The positions of the $L1_0$ FePt 200 and 002 peaks are 48.15° and 49.16° , respectively. Hence, the shift of the peak located between 46° and 50° is due to the shift of the $L1_0$ FePt 002 and 200 peaks. This indicates that the measured FePt lattice parameters are smaller for the thicker Ag underlayer. The c/a ratio of the $L1_0$ FePt, calculated from the deconvoluted FePt 002 and 200 peak positions, also decreases from 0.984 to 0.981 as the Ag underlayer thickness increases from 100 nm to 175 nm. The decreasing lattice parameters of the a and c axes along with the reduced c/a ratio, also indicates that ordering of the $L1_0$ FePt thin films is enhanced by the increased Ag underlayer thickness. This could be due to microstructural changes of Ag underlayer, as shown in Fig. 2.

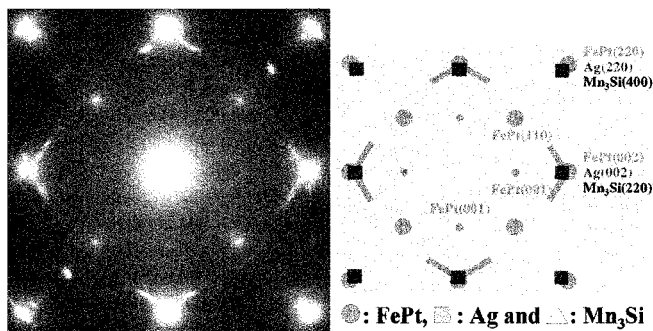


Fig. 4. TEM selected area diffraction pattern of the FePt(30 nm)/Ag(100 nm)/Mn₃Si(400 nm)/Ag(75 nm) thin film.

Because of the excellent lattice match between the Ag (200) and Mn₃Si (200) planes [5], a Mn₃Si layer could be added between two Ag layers. It is conjectured that this may influence the island-like growth of the Ag resulting in a different surface microstructure for the FePt to deposit on. In these films, the total Ag thickness of the FePt/Ag/Mn₃Si/Ag is the same as that of the FePt/Ag(175 nm) film. The TEM bright field images show that the FePt/Ag/Mn₃Si/Ag are continuous thin films. Fig. 4 shows a TEM SAD pattern of the FePt(30 nm)/Ag(100 nm)/Mn₃Si(400 nm)/Ag(75 nm) film. Because the *d*-spacings of the Ag (002) and Mn₃Si (022) planes are very close, the Mn₃Si (200) plane first rotates 45° to grow on the first Ag (200) plane and then the second Ag layer must rotate 45° again to fit on the Mn₃Si (200) plane [5]. The overlap of the FePt(002), Ag(002) and Mn₃Si(220) reflections indicates the similar *d*-spacing of the FePt(002), Ag(002) and Mn₃Si(220) planes. The epitaxial relationship of the FePt/Ag/Mn₃Si/Ag thin films is seen to be FePt(002)[220]||Ag(002)[220]||Mn₃Si(002)[400]||Ag(002)[220]. Very weak L₁₀ FePt 001 reflections are observed in the diffraction pattern, indicating that most of the FePt grains are (001) oriented. Eight streaks are observed in the diffraction pattern along the projection of the <111> directions. These are probably due to stacking faults.

The in-plane and perpendicular magnetic hysteresis loops are shown in Fig. 5. The coercivities for both orientations are higher for FePt(30 nm)/Ag(175 nm) film than those of the FePt(30 nm)/Ag(10 nm) film. As observed, the thicker Ag film produces a smoother and more continuous surface for the FePt film to grow on. Hence, the FePt films should be more exchange coupled. Also, the L₁₀ phase is more predominant for the continuous Ag underlayers. Hence, with thicker Ag, the FePt films should become more exchange coupled, but each grain should have a significantly higher anisotropy. Hence, the thicker Ag underlayer should produce a film with higher coercivity. Compared with FePt/Ag (175 nm) film, the FePt/Ag (10 nm) film shows lower in-plane coercivity due to more disordered phase. Domain wall motion is dominant. Likewise reversible rotation of the magnetization vector is observed when the magnetic field is applied perpendicular to the film plane. This is indicated by the rounded magnetization curve shoulders of the perpendicular hysteresis loop. The open loop coercivity is most likely due to the granular nature of the film and probably represents a regime of wall motion. For the films grown on

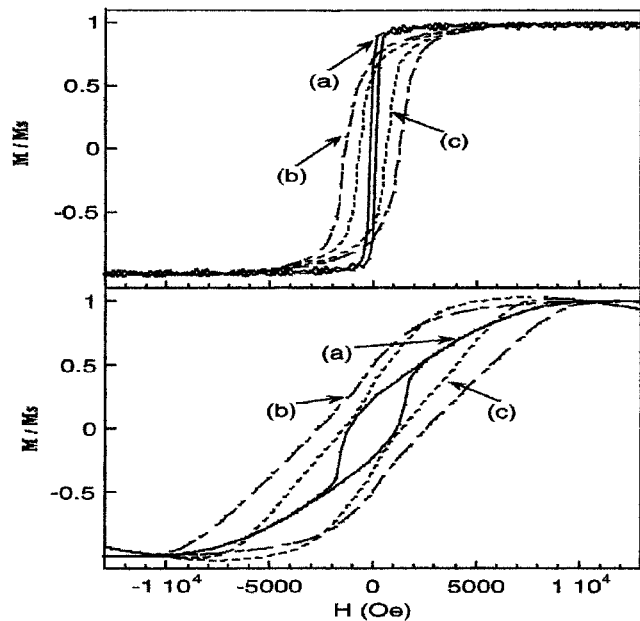


Fig. 5. The in-plane (top) and perpendicular (bottom) hysteresis loops of (a) FePt/Ag(10 nm), (b) FePt/Ag(175 nm) and (c) FePt/Ag/Mn₃Si/Ag thin films.

the thicker Ag, the *c*-axis is more equally distributed along the three cubic axes and so the difference between the in-plane and perpendicular magnetic properties is less pronounced. On the other hand, the in-plane and perpendicular coercivity of the FePt(30 nm)/Ag(100 nm)/Mn₃Si(400 nm)/Ag(75 nm) film is lower than that of the FePt/Ag(175 nm). This may be due to the appearance of the stacking faults in the FePt/Ag/Mn₃Si/Ag film, which has lowered the magneto-crystalline anisotropy energy of the film and reduced coercivity.

IV. CONCLUSION

As the Ag underlayer thickness increases, the Ag microstructure changes from island like to continuous. This results in a change of the microstructural and magnetic properties of the FePt films. The *c* axes of the L₁₀ FePt film deposited onto the 10 nm Ag underlayer are oriented in the film plane. As the Ag thickness increases, the volume fraction of the L₁₀ FePt (001)-oriented grains increases. In addition, the FePt thin film deposited onto the thicker Ag underlayer is more ordered. Compared with the Ag/Si(100) templates, the FePt thin film deposited onto the Ag/Mn₃Si/Ag/Si(001) template are more (001) oriented.

ACKNOWLEDGMENT

The authors gratefully thank Dr. Bin Lu for valuable discussions.

REFERENCES

- [1] R. F. C. Farrow, D. Weller, R. F. Marks, and M. F. Toney, *J. Appl. Phys.*, vol. 79, p. 5967, 1996.
- [2] M. R. Visokay and R. Sinclair, *Appl. Phys. Lett.*, vol. 66, p. 1692, 1995.
- [3] B. M. Lairson, M. R. Visokay, R. Sinclair, and B. M. Clemens, *Appl. Phys. Lett.*, vol. 62, p. 639, 1993.
- [4] W. Yang, D. N. Lambeth, L. Tang, and D. E. Laughlin, *J. Appl. Phys.*, vol. 81, p. 4370, 1997.
- [5] Y.-N. Hsu, D. Laughlin, and D. N. Lambeth, *J. Appl. Phys.*, vol. 87, p. 6698, 2000.